

Colloidal Laves phases as precursors of photonic crystals

Guido Avvisati¹ and Marjolein Dijkstra^{1,*}

¹Debye Institute for Nanomaterials Science, Utrecht University,
Princetonplein 1, 3584CC Utrecht, The Netherlands

(Dated: December 3, 2024)

A considerable amount of research in the colloidal science community deals with the design and fabrication of crystalline phases to be employed as photonic crystals. Here, we propose a novel route to the fabrication of colloidal Laves phases, which can be used as precursors of photonic bandgap structures. We numerically calculate the phase diagram of a binary mixture of hard spheres and hard tetramers, and focus on the stability of the MgCu_2 Laves phase. Our findings show a relatively large coexistence region between the fluid and the Laves phase which is potentially accessible by experiments, uncovering a new self-assembly path towards a photonic structure with a band gap in the visible region.

Keywords: colloidal particles, laves phases, hard tetramers, Monte Carlo methods, free-energy calculations

It is well known that colloidal particles can spontaneously form ordered, periodic phases which are the analogues of crystals in atomic systems. The most prominent example of such a transition, first discovered by computer simulations¹, and later confirmed by experimental work², is the formation of a Face Centered Cubic (FCC) crystal from a fluid of colloidal particles which interact approximately as Hard Spheres (HS).

The study of crystalline phases on colloidal length and time scales is important not only from a fundamental point of view, where it allows for insights into, *e.g.*, phase transitions and crystallisation kinetics^{3,4}, but also for potential applications. In particular, it is possible to fabricate photonic crystals (PCs) from colloidal particles due to the intrinsic size of the employed building blocks. By PCs we mean structures with a periodically varying dielectric constant that display a complete photonic band gap in a given (typically optical) range of frequencies. These structures act for photons in the same way as semiconductors do for electrons, hence opening up a way to control light propagation. The application spectrum of these materials is very broad, ranging from optical fibers, displays and switches to (bio-)sensing and bio-medical engineering, and finally to energy storage and security^{5–8}.

Since the early work on PCs^{9,10}, different particle arrangements have been explored as possible candidates^{11–13}, and some of them – most notably the so called “inverse opals” – have also been fabricated in the lab^{14–18}. To date, the most suitable structures to make PCs certainly remain the diamond crystal (DC) and the pyrochlore structure, in which the colloids are located on the lattice positions of the respective crystal structures¹⁹. However, despite these efforts, the fabrication of such open (non close-packed) structures at the colloidal scales has not yet been achieved, and is a long-standing research focus in the nanomaterials community.

Nevertheless, new perspectives on the subject arise because the recent advances in the colloidal synthesis allow for more and more exotic building blocks to be used

in the colloidal self-assembly arena. Clusters of spheres with well defined shapes, such as dimers, trimers and tetramers, have become available, together with the intriguing possibility of employing them to self-assemble PCs^{20–27}. These colloidal clusters can be produced in several ways. One method takes advantage of the drying forces in an evaporating emulsion droplet to drive the confined colloidal particles to a specific geometry^{20,21,24}. A different class of fabrication procedures relies instead on microfluidics setups, with or without the use of lithographically patterned surfaces.^{26,28–31}.

In addition, on the theoretical side, two new ideas were put forward to possibly facilitate the fabrication of PCs, and we shall briefly discuss them in the following. One study showed that a structure composed of tetrahedral clusters of spheres (“tetrastack”) displays a photonic band gap in the optical region³². However, while they employ a complex building block, it is not clear how the suggested structure can be realised experimentally. Another study suggested that, by using a binary mixture of colloidal particles with different sizes, it is possible to assemble an MgCu_2 Laves phase, from which a DC and a pyrochlore structure can be obtained³³. In this case, the authors address the problem posed by the open structure by using a binary mixtures of spheres. Nevertheless, issues arise when one considers that three distinct Laves phases can actually be assembled from a binary hard-sphere mixture, namely the MgCu_2 , the MgNi_2 , and the MgZn_2 . It is also important to note that the latter is the thermodynamically stable phase, and unfortunately not the aimed MgCu_2 phase³⁴. Furthermore, the three aforementioned Laves phases are nearly degenerate as they have very similar free energies, hence the self-assembly of the mixture often results in glassy states, unless the assembly is directed, *e.g.*, by using templated walls³³.

In this work, we study the phase behaviour of a binary mixture of large hard spheres and rigid, tetrahedral clusters of small hard spheres with a fixed size ratio (hereafter denoted as tetramers). In particular, using

free-energy calculations, we address the thermodynamic stability of the MgCu_2 Laves phase that can result from the self-assembly of the mixture. In this way, we retain the best of both approaches, while circumventing the problems that arise due to the metastability and degeneracy of the three distinct Laves phases. On the one hand, having a binary mixture mitigates the problem of the low-coordinated open target structures, *i.e.*, the diamond and pyrochlore structure that display a photonic bandgap, on the other hand using tetramers as one of the building blocks removes the lattice degeneracy problem at once, as tetramers mimic the local coordination of the pyrochlore structure only in an MgCu_2 lattice. The particular choice of colloidal building blocks intrinsically pre-selects the desired structure, hence the MgCu_2 Laves phase is obtained by design.

We stress that such a model mixture is well within experimental reach, even though no studies on it have been performed yet to the best of our knowledge. This is somewhat surprising as hard-core systems are usually much easier to control than systems with attractive interactions, which often requires substantial fine-tuning of the range, strength, and directionality of the interactions.

In this letter, we consider a binary mixture of N_s large spheres with diameter σ_L and N_t tetramers at composition $x = N_s/N$, with $N = N_s + N_t$. Each tetramer consists of four touching spherical beads of diameter σ_B arranged in a tetrahedral fashion. We assume the tetramers to behave like a rigid body, *i.e.* fluctuations in the geometrical arrangement of the spheres are neglected. The size ratio between a bead in a tetramer and a sphere is denoted as $q = \sigma_B/\sigma_L$. Since the MgCu_2 Laves phase of an ordinary binary hard-sphere mixture achieves the highest packing fraction for $q = \sqrt{2/3} \sim 0.82^{33,34}$, we employ this value in our work. We show a model of the different building blocks in Fig. 1.

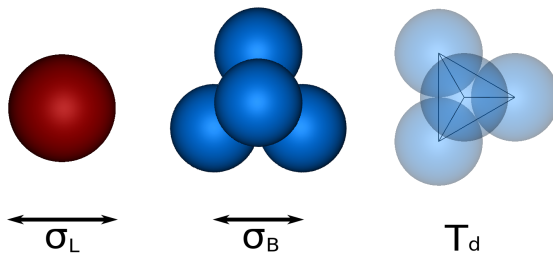


FIG. 1. Building blocks of the investigated binary mixture. (left) Hard spheres with diameter σ_L . (center) Hard tetrahedral tetramers with bead size σ_B . Note that the beads are tangential to one another. The size ratio $q = \sigma_B/\sigma_L$ is fixed to 0.82. (right) Faceted model of tetrahedron, with symmetry group T_d , connecting the centers of the beads.

All interactions are assumed to be HS-like, meaning that the objects do not interpenetrate each other. Hence, the centers of the large hard spheres cannot approach

each other closer than σ_L , the beads of different tetramers cannot approach each other closer than σ_B and the distance between the centers of a large sphere and a bead should always be larger than $\sigma_{LB} = (\sigma_L + \sigma_B)/2$.

In order to map out the phase diagram of this mixture, we perform Monte Carlo (MC) simulations in the isobaric-isothermal ensemble and free-energy calculations. The relevant thermodynamic quantities are N_s, N_t, P, T . The pressure P is measured in reduced units as $\beta P \sigma_L^3$ with $\beta = 1/k_B T$ representing the inverse thermal energy. The number density is given by $\rho \sigma_L^3 = N/V \sigma_L^3$, with V denoting the volume, while the packing fraction is defined as $\eta = \gamma \rho$, with $\gamma = \pi \sigma_L^3 [x + 4q^3(1-x)]/6$. For each composition x , the equation of state (EOS) is computed by means of compression and expansion runs. For the compression runs, the starting configuration is a disordered fluid of $N_s = xN$ spheres and $N_t = (1-x)N$ tetramers. For the expansion runs, crystalline structures with the composition determined by the crystal stoichiometry provide the initial configuration as explained in the following.

For a binary hard-sphere mixture, previous studies have shown that, at the chosen size ratio $q = \sigma_S/\sigma_L = 0.82$, only three crystal structures are stable over the entire composition x range^{33,34}, namely the FCC crystals of pure large and pure small spheres, and the Laves phases. In the case of a mixture of tetramers and spheres, we employ the same packing arrangements as those in Ref. [34], but we replace every four small spheres by a tetramer. This procedure yields structures which are made from the investigated building blocks (spheres and tetramers), but are arranged similarly to the respective literature cases. In summary, for different compositions x we have:

- SC, a simple cubic lattice of tetramers with a fixed orientation at composition $x = 0$.
- Laves phase, a binary crystal of tetramers and spheres, with the same packing arrangement as the MgCu_2 phase, at composition $x = 2/3$.
- FCC, the thermodynamic stable structure for large hard spheres, at composition $x = 1$.

A graphical overview of the investigated crystal structures is given in Fig. 2. In the simple cubic crystal of tetramers and the Laves phase respectively, all the tetramers have the same orientation, which is calculated by a rigid transformation of the bead positions in the reference frame to the bead positions in the crystal at hand. We note that other arrangements are, in principle, possible for the simple cubic phase, with respect to both positions and orientations of the tetramers, nevertheless the position of the beads of the tetramers must always be compatible with an FCC packing. Moreover, the degeneracy of the SC phase, if present at all, is expected to be small³⁵, hence we neglect it in our calculations.

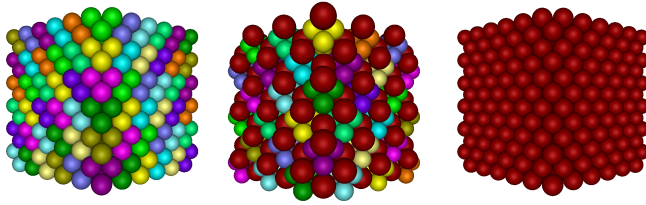


FIG. 2. Crystal structures considered in this work. (left) Simple Cubic crystal of pure tetramers (SC) at composition $x = 0$. (center) binary MgCu_2 Laves phase at composition $x = 2/3$. (right) Face Centered Cubic of pure large spheres (FCC) at composition $x = 1$. The color code identifies different tetramers and distinguishes tetramers from spheres.

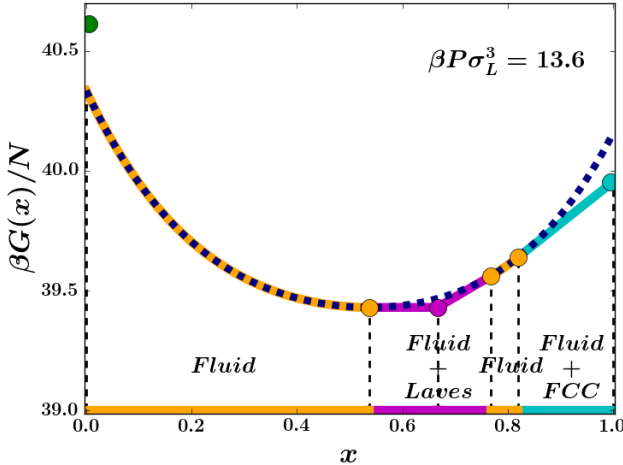


FIG. 3. Gibbs free energy per particle $g = \beta G(P, x)/N$ as function of composition $x = N_s/N$ for a fixed pressure $\beta P \sigma_L^3 = 13.6$. The green, magenta and cyan dots represent the SC phase of pure tetramers (at $x = 0$), the Laves phase (at $x = 2/3$), and the FCC of pure large spheres (at $x = 1$), respectively. The blue dashed line shows the Gibbs free energy $g(P, x)$ of the fluid as function of composition x . The orange dots represent the coexistence points between fluid and Laves phase (2 points) and between fluid and the FCC crystal of pure large spheres as calculated by the common tangent construction. The thick lines show the path of minimal gibbs free energy.

The phase diagram is determined by using the common tangent construction to the Gibbs free energy g curve as a function of the composition x . The dimensionless Gibbs free energy per particle is defined as $g = \beta G/N = f + Z$, where $f = \beta F/N$ is the dimensionless Helmholtz free energy per particle and $Z = \beta P/\rho = \gamma \beta P/\eta$ is the compressibility factor. Starting from a reference f , and assuming no first-order phase transition line is crossed along the integration path, the Gibbs free energy g can be written as

$$g(P, x) = f(\eta_0, x) + \gamma \int_{\eta_0}^{\eta} d\eta' \frac{\beta P(\eta', x)}{\eta'^2} + Z(P, x) \quad (1)$$

The main problem is now shifted to the computation of f at the reference point. For the fluid phase we choose this point to be an ideal gas mixture, whereas we use the Frenkel-Ladd method and its extension that takes into account the anisotropic particle shape in the case of the crystal phases^{36–38}. More details on this method can be found in Ref. [38] and references therein.

Using Eq. 1, we calculate the Gibbs free energy $g(P, x)$ for the fluid phase at different compositions x with a grid spacing of 0.1, as well as the $g(P, x)$ for the solid phases. We then use the common tangent construction in the (g, x) -plane to draw the phase diagram. A representative calculation of $g(P, x)$ is given in Fig. 3, where we also show the results of the common tangent construction.

To draw the phase diagram in the pressure $\beta P \sigma_L^3$ -composition x representation, we collect all the information from the calculations of $g(P, x)$ at different pressures, namely all the coexistence points between the different phases. The results are summarised in Fig. 4.

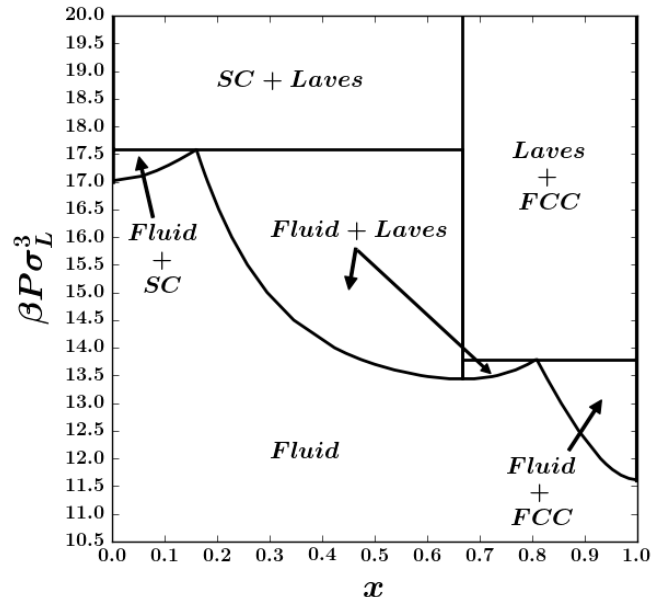


FIG. 4. Phase diagram of a binary mixture of hard spheres and hard tetramers in the pressure $\beta P \sigma_L^3$ -composition x representation. The composition x refers to the spheres. Two triple points (Fluid+SC+Laves, Fluid+Laves+FCC) are found, together with a relatively large phase coexistence region between fluid and Laves phase.

For pressures $\beta P \sigma_L^3 \leq 11.5$, we find that the fluid is the only stable phase. Increasing the pressure results in different coexistence regions, between the fluid and the three crystal structures investigated, and between the different crystal structures at even higher pressures.

For $11.5 \leq \beta P \sigma_L^3 \leq 13.9$ and compositions $x > 0.81$ we find coexistence between the FCC crystal of large spheres and the fluid phase, while for $17.0 \leq \beta P \sigma_L^3 \leq 17.6$ and compositions $x < 0.17$ we find a coexistence between the simple cubic crystal of tetramers and the fluid phase.

Interestingly, at intermediate pressures and compositions we observe two distinct phase coexistence regions between the Laves phase and the fluid phase with either a composition smaller or larger than that of the Laves phase, *i.e.*, $x \leq 2/3$ and $x \geq 2/3$. Moving towards high pressures we find solid-solid coexistence between the simple cubic phase of pure tetramers and the Laves phase, and between the Laves phase and the pure FCC phase of large spheres, the former starting at somewhat higher pressures than the latter ($\beta P \sigma_L^3 > 17.6$ vs $\beta P \sigma_L^3 > 13.9$).

For very high pressures, we expect only a single coexistence region between the simple cubic phase of tetramers and the FCC crystals of large spheres, due to packing considerations. However, we were unable to detect the crossover, even by simulating at pressures as high as $\beta P \sigma_L^3 = 30.0$. Thus, we can only set a lower limit on this specific crystal-crystal phase coexistence region.

The relatively large two-phase coexistence region between the fluid phase and the Laves phase is the most remarkable feature of the presented phase diagram, signalling an extended and easily accessible parameter range to obtain the targeted MgCu_2 Laves phase in simulations as well as in experiments. We checked this result by additionally performing direct coexistence simulations at overall concentrations $x = 0.5$ and $x = 0.6$ and pressure $\beta P \sigma_L^3 = 15.0$. In Fig. 5 we present snapshots of the final configurations as obtained from the simulations, which confirm the coexistence between the fluid phase and the Laves phase of tetramers and spheres.

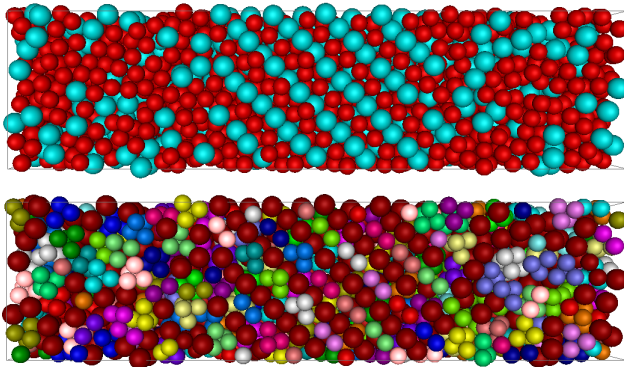


FIG. 5. Representative final configuration from direct coexistence simulations displaying coexistence between the fluid phase and the Laves crystal of hard tetramers and hard spheres. (top) Composition $x = 0.6$ and pressure $\beta P \sigma_L^3 = 15.0$. (bottom) Same as top panel, but with color coding as to highlight the different tetramers.

Despite the progress in the fabrication of colloidal building blocks, we are unaware, to the best of our knowledge, of experimental realisations of the proposed binary mixture. In order to facilitate the comparison with experimental results we additionally convert the phase diagram to the packing fraction of tetramers η_T – packing fraction of spheres η_S representation, the result being shown in

Fig. 6. The triple points we found in Fig. 4 – Fluid + SC + Laves, Fluid + Laves + FCC – transform to triangular areas in this representation. In between the triple points we find the coexistence region between fluid phase and Laves structure, which could be probed experimentally.

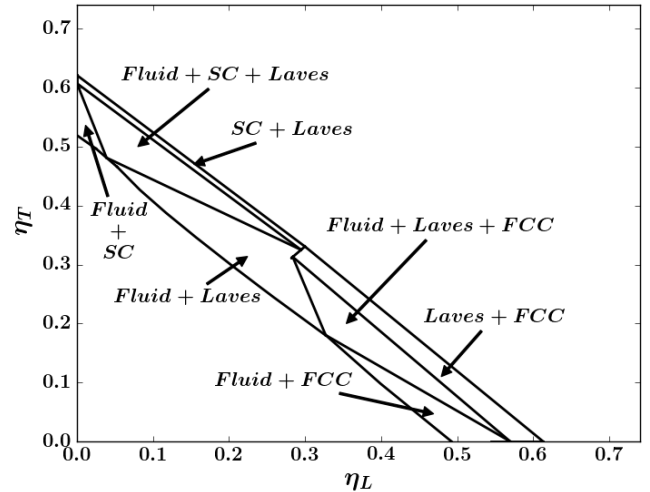


FIG. 6. Phase diagram of the investigated binary mixture in the packing fraction of tetramers η_T – packing fraction of large spheres η_L representation.

To summarise, We have investigated the phase behaviour of a binary mixture of hard spheres and hard tetramers with beads arranged in a tetrahedral fashion.

We found two-phase coexistence regions between the fluid phase and the various crystal structures, as well as two triple points, namely the Fluid+SC+Laves and the Fluid+Laves+FCC triple points. Surprisingly, we find a relatively large coexistence region between the fluid and the Laves phase – the structural analogue of the conventional MgCu_2 Laves phase, which may be experimentally accessible.

Additionally, we converted the phase diagram from the pressure $\beta P \sigma_L^3$ – composition x representation to the packing fraction of tetramers η_T – packing fraction of spheres η_L plane, in order to facilitate comparison with experimental parameters.

Our simulation results demonstrate a novel self-assembly route towards a photonic crystal, in which the diamond structure and the pyrochlore structure can be assembled in one crystal – the MgCu_2 Laves structure – from a binary mixture of hard spheres and hard tetramers. By selectively burning or dissolving one of the species, either the tetramers or the spheres, the Laves phase can be converted into a diamond lattice or a pyrochlore structure to obtain a photonic crystal with a bandgap in the visible range. We hope that our results will stimulate further experimental and theoretical investigations. In future work, we will address the crystallization kinetics of the proposed self-assembly route, as well as the effect of gravity and colloidal epitaxy.

ACKNOWLEDGEMENTS

This work is part of the research programme of the Foundation for Fundamental Research on Matter (FOM), which is part of the Netherlands Organisation for Scientific Research (NWO). M.D. acknowledges financial support from a NWO-VICI grant. G.A. thanks L. Filion, S. Dussi and T. Dasgupta for fruitful discussions. The authors thank H. Patabhiraman and V. Prymidis for critically reading the manuscript.

* m.dijkstra@uu.nl

- [1] B. J. Alder and T. E. Wainwright, *The Journal of Chemical Physics* **27**, 1208 (1957).
- [2] P. N. Pusey and W. van Megen, *Nature* **320**, 340 (1986).
- [3] P. J. Lu and D. A. Weitz, *Annual Review of Condensed Matter Physics* **4**, 217 (2013).
- [4] B. Li, D. Zhou, and Y. Han, *Nature Reviews Materials* **1**, 15011 (2016).
- [5] A. Stein, B. E. Wilson, and S. G. Rudisill, *Chem. Soc. Rev.* **42**, 2763 (2013).
- [6] G. von Freymann, V. Kitaev, B. V. Lotsch, and G. A. Ozin, *Chem. Soc. Rev.* **42**, 2528 (2013).
- [7] J. Xu and Z. Guo, *Journal of Colloid and Interface Science* **406**, 1 (2013).
- [8] J. Ge and Y. Yin, *Angewandte Chemie International Edition* **50**, 1492 (2011).
- [9] V. P. Bykov, *Soviet Journal of Quantum Electronics* **4**, 861 (1975).
- [10] E. Yablonovitch, *Phys. Rev. Lett.* **58**, 2059 (1987).
- [11] K. M. Ho, C. T. Chan, and C. M. Soukoulis, *Phys. Rev. Lett.* **65**, 3152 (1990).
- [12] K. Ho, C. Chan, C. Soukoulis, R. Biswas, and M. Sigalas, *Solid State Communications* **89**, 413 (1994).
- [13] S. G. Johnson and J. D. Joannopoulos, *Applied Physics Letters* **77**, 3490 (2000).
- [14] S.-Y. Lin, J. Fleming, D. Hetherington, B. Smith, R. Biswas, K. Ho, M. Sigalas, W. Zubrzycki, S. Kurtz, and J. Bur, *Nature* **394**, 251 (1998).
- [15] J. E. G. J. Wijnhoven and W. L. Vos, *Science* **281**, 802 (1998).
- [16] R. C. Schrodin, M. Al-Daous, C. F. Blanford, and A. Stein, *Chemistry of Materials* **14**, 3305 (2002).
- [17] Y. A. Vlasov, X.-Z. Bo, J. C. Sturm, and D. J. Norris, *Nature* **414**, 289 (2001).
- [18] M. Qi, E. Lidorikis, P. T. Rakich, S. G. Johnson, J. D. Joannopoulos, E. P. Ippen, and H. I. Smith, *Nature* **429**, 538 (2004).
- [19] E. C. M. Vermolen, J. H. J. Thijssen, A. Moroz, M. Megens, and A. van Blaaderen, *Opt. Express* **17**, 6952 (2009).
- [20] V. N. Manoharan, M. T. Elsesser, and D. J. Pine, *Science* **301**, 483 (2003).
- [21] C. Young-Sang, Y. Gi-Ra, K. Shin-Hyun, D. J. Pine, and Y. Seung-Man, *Chemistry of Materials* **17**, 5006 (2005).
- [22] D. J. Kraft, J. Groenewold, and W. K. Kegel, *Soft Matter* **5**, 3823 (2009).
- [23] C. Liddell and C. Summers, *Advanced Materials* **15**, 1715 (2003).
- [24] S.-M. Yang, S.-H. Kim, J.-M. Lim, and G.-R. Yi, *J. Mater. Chem.* **18**, 2177 (2008).
- [25] Y. Lu, Y. Yin, and Y. Xia, *Advanced Materials* **13**, 415 (2001).
- [26] J.-T. Wang, J. Wang, and J.-J. Han, *Small* **7**, 1728 (2011).
- [27] S. Sacanna and D. J. Pine, *Current Opinion in Colloid & Interface Science* **16**, 96 (2011).
- [28] Y. Yin and Y. Xia, *Advanced Materials* **13**, 267 (2001).
- [29] Y. Xia, Y. Yin, Y. Lu, and J. McLellan, *Advanced Functional Materials* **13**, 907 (2003).
- [30] L.-Y. Chu, A. Utada, R. Shah, J.-W. Kim, and D. Weitz, *Angewandte Chemie International Edition* **46**, 8970 (2007).
- [31] E. Duguet, A. Desert, A. Perro, and S. Ravaine, *Chem. Soc. Rev.* **40**, 941 (2011).
- [32] T. T. Ngo, C. M. Liddell, M. Ghebrebrhan, and J. D. Joannopoulos, *Applied Physics Letters* **88**, 241920 (2006).
- [33] A.-P. Hyyninen, J. H. Thijssen, E. C. Vermolen, M. Dijkstra, and A. Van Blaaderen, *Nature Materials* **6**, 202 (2007).
- [34] A.-P. Hyyninen, L. Filion, and M. Dijkstra, *The Journal of Chemical Physics* **131**, 064902 (2009).
- [35] M. Kowalik, K. Tretiakov, and K. Wojciechowski, *Computational Methods in Science and Technology* **16**, 141 (2010).
- [36] D. Frenkel and B. Smit, *Understanding Molecular Simulation: From Algorithms to Applications (Computational Science)*, 2nd ed. (Academic Press, 2001).
- [37] D. Frenkel and A. J. C. Ladd, *The Journal of Chemical Physics* **81**, 3188 (1984).
- [38] C. Vega, E. Sanz, J. L. F. Abascal, and E. G. Noya, *Journal of Physics: Condensed Matter* **20**, 153101 (2008).